

# EFFECTS OF TRANSVERSE PHYSICS ON NONLINEAR EVOLUTION OF LONGITUDINAL SPACE-CHARGE WAVES IN BEAMS \*

K. Tian<sup>1#</sup>, I. Haber<sup>2</sup>, R. A. Kishek<sup>2</sup>, P. G. O'Shea<sup>2</sup>, M. Reiser<sup>2</sup>, D. Stratakis<sup>3</sup>

<sup>1</sup>Thomas Jefferson National Accelerator Facility, Newport News, 23606

<sup>2</sup>IREAP, University of Maryland, College Park, MD 20742

<sup>3</sup>Brookhaven National Laboratory, Upton, NY 11973

## Abstract

Longitudinal space-charge waves can introduce energy perturbations into charge particle beams and degrade the beam quality, which is critical to many modern applications of particle accelerators. Although many longitudinal phenomena arising from small perturbations can be explained by a one-dimensional cold fluid theory, nonlinear behavior of space-charge waves observed in experiments has not been well understood. In this paper, we summarize our recent investigation by means of more detailed measurements and self-consistent simulations. Combining the numerical capability of a PIC code, WARP, with the detailed initial conditions measured by our newly developed time resolved 6-D phase space mapping technique, we are able to construct a self consistent model for studying the complex physics of longitudinal dynamics of space-charge dominated beams. Results from simulation studies suggest that the unexplained nonlinear behavior of space-charge waves may be due to transverse mismatch or misalignment of beams.

## INTRODUCTION

As a result of growing interest in intense beam applications such as accelerator-driven high-energy-density physics (HEDP) [1], pulsed neutron sources [2], and x-ray free electron lasers [3], a detailed knowledge and understanding of space-charge dominated beams has become increasingly important for the successful operation of such machines. For these machines, near the source, longitudinal space-charge waves can be generated by a density perturbation or energy perturbation. Such perturbations can lead to instabilities that can disrupt the beam under certain circumstances. Much effort has been made for studying space-charge dominated beams experimentally; for example, the High Current Experiment (HCX) [4] and the Paul Trap Simulator Experiment (PTSX) [5]. Since early 1990s, the charged particle beams group at University of Maryland has carried out numerous experimental studies on longitudinal space-charge waves by deliberately introducing localized density or energy modulations into highly intense electron beams [6]. The earlier investigations reveal much about the evolution of space-charge waves. However, there was no clear explanation for the unexpected experimental result in the nonlinear regime, where the 1-D linear theoretical model breaks down [7]. Another issue with the

previous studies is their neglect of the transverse distribution and its effect on the longitudinal dynamics.

Since the initial conditions of the beam are critical to accurate simulation of the beam behavior, we need experimental characterization of the initial beam for both perturbed and unperturbed beams. The typical width of the perturbation is only about 10 ns, therefore the measurements must resolve that timescale. Previously, we have measured for the first time both detailed energy profiles [6], and time resolved transverse distributions [8] of space-charge waves. These results have informed on the correlations between the transverse and longitudinal beam distributions. More importantly, these measurements were critical for initializing self-consistent computer models. In this paper, we present new findings on the evolution of space-charge waves derived both from experimental measurement and numerical simulations.

## EXPERIMENTAL METHOD

The Long Solenoid Experiment (LSE) at University of Maryland consists of an electron gun [9], four short solenoids, and a 1.5 m long solenoid. The system, shown in Fig. 1, contains three Bergoz current monitors with a time resolution of 200 ps, two high resolution energy analyzers [7], and two phosphor screens.

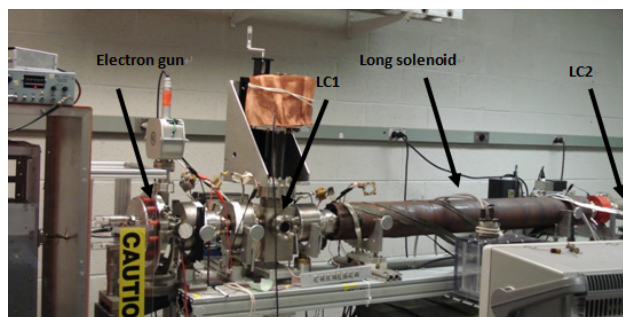


Figure 1: A photo of the upgraded LSE system.

The two energy analyzers are inside two diagnostics chambers LC1 and LC2, which are located 43.5 cm and 234 cm away from the gun aperture. The positions of the magnets and other diagnostics are listed in Table 1 as the distance in cm from the center of the solenoids (S1-S5), and Bergoz current monitors (B1-B3) to the downstream edge of the gun aperture.

We managed to obtain different current profiles with both negative and positive initial perturbations [9]. For all beams, the strengths of solenoids were chosen to match unperturbed beams into the long solenoid with a matched

\*Work supported by US Department of Energy, the office of Naval Research and the Joint Technology Office.

<sup>#</sup>kaitian@umd.edu

beam radius of 4.9 mm. When the bias voltage  $V_b$  was set to 30 V, the polarities of the current perturbations were found to be negative. On the other hand, when the bias voltage was increased to 52 V, positive perturbations were introduced to the main beam current. The main beam current  $I_0$ , initial current perturbation strength  $\eta$ , defined as the ratio of perturbation current  $I_1$  and  $I_0$ , and main beam energy  $E_0$  are 94.5 mA, -0.08, and 5075 eV respectively when  $V_b=30$ V; they are 69.8 mA, 0.32, and 5053 eV, respectively when  $V_b=52$ V.

Table 1: Magnets and Current Monitor Positions

S1	S2	S3	S4	S5	B1	B2	B3
11.0	29.0	55.0	136.0	217.0	18.5	63.0	207.0

Current profiles of all beams are measured by the three Bergoz current monitors (B1, B2, and B3) and are shown in Fig. 2, where current profiles measured by B2 and B3 are shifted up by 10 mA and 20 mA, respectively, in (a), and by 20 mA and 40 mA, respectively, in (b). In Fig. 3, current profiles obtained at different locations and the mean energy profiles at LC1 and LC2 are plotted for both cases. The full beam length is about 100ns, but since we are focused on the perturbations, the beam head and tail are not shown in these figures.

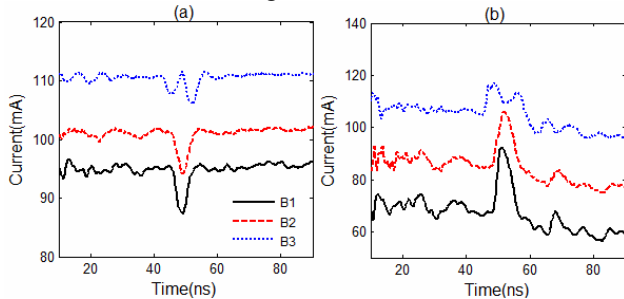


Figure 2: (color): Current profiles of the 4.9 mm beams when the bias voltage was set to (a) 30 V and (b) 52 V.

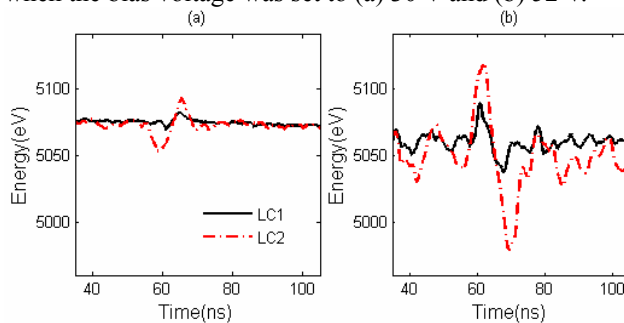


Figure 3: (color): Mean energy profiles measured at LC1 and LC2 (a)  $V_b=30$  V and (b)  $V_b=52$  V.

Using the measured energy profiles in LC1 and current profiles by B1, we solve the 1-D cold fluid model to predict the energy profile in LC2. The comparison for case (b) shows that the measured energy perturbation in LC2 is much smaller than the theoretical prediction. For case (b), we also observed beam loss inside the long solenoid by comparing the current profiles measured by different current monitors [9]. Hence, we set up numerical

simulations to investigate the cause and effect of the beam loss.

## SIMULATION RESULTS

In this section, we apply the particle-in-cell-code WARP [10] to model the experiment, using the experimental data upstream to initialize the simulation, and compare the output to the experimental data downstream. To investigate the nonlinear phenomena of space-charge waves, we apply the lab-frame WARP model to a rectangular perturbed beam, which has a main beam current of 40 mA and a peak perturbation current of 47.6 mA. Similar to the 69.8 mA beam in the last section, the measured energy perturbation of this beam in LC2 has a very large discrepancy from 1-D theory [9].

The transport channel in WARP consists of 4 solenoids starting from LC1. The strengths of the solenoids are set to be consistent with those used in experiments. We inject only a beam 40 ns long with the perturbation at center to improve the efficiency of computation. The beam current, transverse radius, and the energy of the injected particles are adjusted to values measured in experiment. All these measured profiles and numerical settings for simulations can be found in Ref. [8].

In WARP, we are able to insert a virtual conducting tube concentric with the beam pipe. This tube does not affect the field solving during simulation, but catch those particles wandering beyond a certain boundary, i.e. the wall radius. Fig. 4 illustrates two different wall radii that were used in the simulation using a snapshot of the beam at  $t=57.2$  ns. As our simulation is in RZ geometry, the projection of the particle distribution in X-Z plane is equivalent to that in the R-Z plane. The units of both axes are meter. The perturbation is located from 1.22 m to 1.7 m.

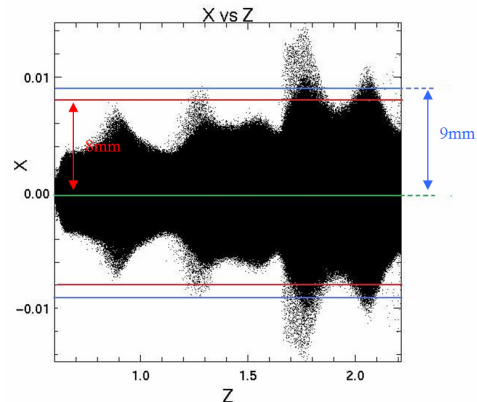


Figure 4(color): Illustration of applying two virtual conducting tubes in WARP code.

The simulation results of current and energy profiles are presented in Fig. 5, where  $r_w$  represents the radius of the virtual tube. When  $r_w=1.9$  cm, the virtual tube has the same radius as the beam pipe, thus the simulation result is the same as what we have presented earlier. The current profile becomes close to the experimental result when  $r_w$

=9 mm. At the same time, although the energy profile in this case still has a significant larger modulation than the experimental result, it is much closer compared with the simulation without any beam loss. If the radius of the virtual tube is further cut down to 8 mm, we obtain an energy profile that is very similar to the experimental result. However, the current loss is more than the experiment in this case.

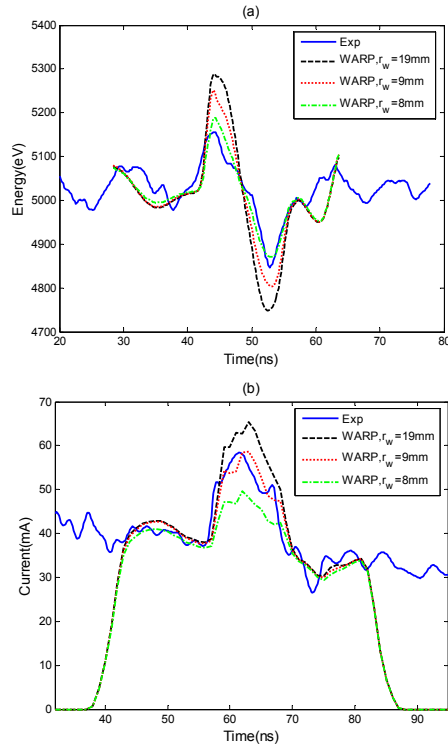


Figure 5(color): Comparison of results from the experiment, WARP simulations with different radii of the virtual tube: (a): Mean energy profiles at LC2; (b) Current profiles at B3.

We believe that there are two possible reasons for why we cannot get the agreement with the current and energy profiles at the same time. First, in experiment, the beam loss may occur earlier than that in the simulation. Thus, for losing the same amount of particles, the longitudinal field is damped earlier in experiment. As a result, we obtain a smaller energy modulation from the experimental measurement. Second, in practice the beam loss may be caused by the mismatch or misalignment, which can offset the beam from the center of the pipe. As discussed in Ref. [11], the longitudinal self electric field is proportional to  $g \frac{\partial \Delta}{\partial z}$ . When the beam is off center, the  $g$ -factor may become different and probably smaller because of the non-uniform field of image charges. To better understand the role of the  $g$ -factor here, more studies are required.

Finally, we also conducted the sensitivity study of this 40 mA beam. The WARP simulation results are not sensitive to the change of initial beam radius, emittance,

slope, and energy. Due to the lack of a theoretical model for the evolution of nonlinear perturbations, it is difficult to judge if the beam loss is the only reason for the nonlinear effects. Other factors, such as the transient behavior of the energy analyzer and the longitudinal-transverse coupling, should also be investigated as future work.

## CONCLUSIONS

The upgrade LSE system enabled us to obtain a complete set of experimental data for both current and energy profiles of the space-charge waves. For the beam with an extremely large perturbation, we observed a large discrepancy between the experimental results and those from the simulation. Further simulation studies suggest that the beam loss due to mismatch or misalignment can contribute to inconsistent results between the experiment and simulation.

Recently, by employing the tomography technique, we have constructed the time-resolved phase space with a resolution of 3 ns [12]. In future, it is necessary to carry out a full 3-D beam frame simulation using the measured 6-D phase space distribution as initial conditions. They can help us simulate the mismatch of the nonlinear perturbation more accurately, and test sensitivity to misalignment. They may also provide some clues about the beam loss and its relationship with  $g$ -factor.

## ACKNOWLEDGEMENT

We wish to acknowledge Y. Zou, Y. Cui, M. Walter, S. Bernal, B. L. Beaudoin, D. Sutter, D. Cohen, D. Feldman, R. Fiorito, J. C. T. Thangaraj, and C. Wu for helpful discussions. We also want to thank A. Friedman, D.P. Grote, and J.-L. Vay providing the WARP codes. This work is supported by the US Department of Energy grant numbers DE-FG02-94ER40855 and DE-FG02-92ER54178, and by the Office of Naval Research and the Joint Technology Office.

## REFERENCES

- [1] A. Friedman, J. J. Barnard, D. P. Grote *et al.*, Proc. 2005 Part. Accel. Conf.
- [2] R.F. Welton, *et al.*, Rev. Sci. Instrum. **75**, 1793(2004)
- [3] C.A. Brau, Free-Electron Lasers (Academic Press, San Diego, 1990).
- [4] P. A. Seidl, D. Baca, F. M. Bieniosek *et al.*, Proc. 2003 Part. Accel. Conf.
- [5] E. P. Gilson, *et al.*, Phys. Rev. Lett. **15**, 155002 (2004).
- [6] K. Tian, *et al.*, Phys. Rev. ST Accel. Beams **9**, 014201 (2006) and references therein.
- [7] Y. Zou, *et al.*, Phys. Rev. Lett. **84**, 5138 (2000).
- [8] K. Tian, *et al.*, Phys. Plasmas **15**, 056707(2008).
- [9] K. Tian, Ph.D dissertation, 2008.
- [10] D. P. Grote, *et al.*, Fusion Eng. Des **32-33**, 193 (1996).
- [11] M. Reiser, Theory and Design of Charged Particle Beams, Wiley: New York (1994).
- [12] D. Stratakis, *et al.*, Proc. 2009 Part. Accel. Conf.